IDENTIFYING GAMMA-RAY BURST REMNANTS THROUGH POSITRON ANNIHILATION RADIATION

Steven R. Furlanetto & Abraham Loeb
Harvard-Smithsonian Center for Astrophysics, 60 Garden St., Cambridge, MA 02138;
sfurlanetto@cfa.harvard.edu, aloeb@cfa.harvard.edu

Draft version March 5, 2002

ABSTRACT

We model the annihilation of relic positrons produced in a gamma-ray burst (GRB) after its afterglow has faded. We find that the annihilation signal from at least one GRB remnant in the Milky Way galaxy should be observable with future space missions such as INTEGRAL and EXIST, provided that the gas surrounding the GRB source has the typical density of the interstellar medium, $\lesssim 1$ cm^{-3}. Three fortunate circumstances conspire to make the signal observable. First, unlike positrons in a standard supernova, the GRB positrons initially travel at a relativistic speed and remain ahead of any non-relativistic ejecta until the ejecta become rarefied and the annihilation time becomes long. Second, the GRB remnant remains sufficiently hot ($T \gtrsim 5 \times 10^5$ K) for a strong annihilation line to form without significant smearing by three-photon decay of positronium. Third, the annihilation signal persists over a time longer than the average period between GRB events in the Milky Way galaxy.

Subject headings: gamma rays: bursts – supernova remnants – X-rays: ISM

1. INTRODUCTION

The detailed nature of the central engine of gamma-ray bursts (GRBs) is still unknown (van Paradijs, Kouveliotou, & Wijers 2000; Piran 2000, and references therein). Attempts to derive empirical constraints on the environment (Djorgovski et al. 2001, and references therein), the frequency (Schmidt 2001), the collimation angles and energy output (Frail et al. 2001; Freedman & Waxman 2001; Panaitescu & Kumar 2001b; Piran et al. 2001) or the possible association of GRBs with supernovae (Bloom et al. 1999; Kulkarni et al. 2000; Reichart 2001) are compromised by the difficulty of observing GRBs across large cosmological distances. Obviously, identification of old GRB remnants in the local universe would provide much better insight into the nature of GRB progenitors (Loeb & Perna 1998; Woods & Loeb 1999; Perna, Raymond & Loeb 2000; Paczynski 2001; Ayal & Piran 2001).

Given the recently inferred similarity between the energy output in supernovae and GRBs, $\sim 10^{51}$ ergs (Frail et al. 2001), it now appears difficult to separate the late evolution stages of their remnants hydrodynamically. Even if a GRB explosion is initially highly beamed, the asymmetry of the blast wave it generates in the surrounding interstellar medium (ISM) would be erased on an isotropization timescale $t_{\rm iso} \sim 6 \times 10^3 (E_{51}/n_0)^{1/3}$ yr (Ayal & Piran 2001), where E_{51} is the kinetic energy output of the GRB in units of 10^{51} erg and $n_0 = \rho_{\rm ISM}/\mu_b m_p$ is the ambient number density of atoms in units of cm^{-3} for a mean molecular weight $\mu_b = 1.4$. Subsequently, the blast wave expands just as in a normal supernova (SN) remnant. Any non-relativistic, SN-like ejecta would moderate the initial GRB asymmetry as soon as it overtakes the decelerating GRB shock (Piran & Ayal 2002). External anisotropy may also result from the interaction of the remnant blast wave with a non-uniform ISM. Thus, morphological studies alone cannot unambiguously identify GRB remnants. The alternative method of seeking spectral signatures of the photoionized regions around GRBs (Perna, Raymond, & Loeb 2000) also suffers from potential confusion with SNe occurring in unusual environments.

In this *Letter*, we point out that positrons produced during the early relativistic GRB phase offer a powerful tool for identifying GRB remnants. We model the expansion of a GRB remnant and show that a well-defined annihilation line should be visible until radiative cooling becomes important, at which time the remaining positrons annihilate rapidly (see also Dermer & Böttcher 2000).

2. MODEL OF GRB REMNANTS

We model the initial GRB explosion as two highly-relativistic jets of material moving in opposite directions, initially covering a fraction f_b of a sphere surrounding the GRB. We assume that a fraction ξ_+ of the GRB energy is transformed into e^+ *rest mass*. The positrons can either be produced during the burst itself (Cavallo & Rees 1978; Shemi & Piran 1990) or by interactions of the γ-rays with the ambient medium (Thompson & Madau 2000; Dermer & Böttcher 2000; Mészáros, Ramirez-Ruiz, & Rees 2001). We scale our results to a fiducial value of $\xi_{-2.3} = (\xi_+/0.005)$ corresponding to half of the GRB energy in positrons with a bulk Lorentz factor $\gamma \sim 100$ as required by the compactness argument (Piran 2000). We therefore assume a total of $N_+ = 6 \times 10^{54} \xi_{-2.3} E_{51}$ positrons in the GRB.

The positrons initially travel at a relativistic speed just ahead of the GRB jet. The jet begins to decelerate when it reaches a radius $R_j \sim 0.2 (E_{51}/n_0)^{1/3}$ pc (Rhoads 1997). At this point, it begins to expand sideways and slows exponentially to non-relativistic speeds. Thereafter, simulations have shown that $R_j \propto t^{1/3}$ until the remnant isotropizes at $t_{\rm iso}$ and begins a Sedov-Taylor spherical expansion (Ayal & Piran 2001).

If the commonly hypothesized link between GRBs and SNe exists, then the jet will be followed by SN ejecta of mass $M_{\rm ej} \sim 10\,{\rm M}_\odot$. The ejecta expand freely behind the jet and eventually impact the (decelerating) positrons at a time $t_{\rm mix} \sim 110 (E_{51}/n_0)^{1/3} v_4^{-3/2}$ yr, where v_4 is the ejecta velocity in units of 10^4 km s^{-1} (Piran & Ayal 2002). At this point, the density is $n_{\rm mix} \gtrsim$

$50 M_1 (n_0/E_{51}) v_4^{3/2}$ cm^{-3}, assuming that the ejecta are distributed uniformly throughout the remnant and where $M_1 = (M_{\rm ej}/10\ {\rm M}_\odot)$. If mixing of the ejecta and shocked gas is efficient, then the ejecta-dominated expansion models of Truelove & McKee (1999) show that by this point the thermal energy imparted to the swept-up material could heat the remnant to a temperature $T_{\rm mix} \gtrsim 10^8$ K (E_{51}/M_1). The ratio of the annihilation time to remnant age does not change with time, $\tau_{\rm ann}/t \sim 500 M_1^{-1} (E_{51}/n_0) v_4^{-3/2}$. Thus, only a small fraction of the positrons should annihilate during this very early stage, even if the ejecta are concentrated in a shell of width $\sim 0.1 R_{\rm mix}$.

This contrasts with the survival of positrons in a standard SN, where a substantial number of positrons can be created through the decay chain $^{56}{\rm Ni} \rightarrow ^{56}{\rm Co} \rightarrow ^{56}{\rm Fe} + e^+$, which has a decay time of $\tau \sim 111$ days and occurs for 18% of the ^{56}Ni atoms. [In SN1987A, observations imply that $\sim 2.6 \times 10^{53}$ e^+ were produced through this channel (Suntzeff & Bouchet 1990).] The SN positrons are produced inside the cool, dense SN ejecta when $\tau_{\rm ann}/t \lesssim 0.03$ (depending on the uncertain ionization and temperature structure of the ejecta). Therefore, most of the SN positrons are annihilated within a few years of the SN explosion. Milne, The, & Leising (1999) have confirmed numerically that only a small fraction of the positrons can escape the initial stages of the remnant evolution in Type Ia SNe.

After passing through the external shock most positrons will rapidly thermalize with the ambient medium while a small fraction ($\sim 10^{-3}$) will be re-accelerated by the (collisionless) external shock (Gieseler, Jones, & Kang 2000). If positrons are produced ahead of the shock, then they will have a characteristic Lorentz factor $\gamma_+ \sim 30$ (Mészáros et al. 2001). Regardless of their initial state, the positrons cool rapidly through Coulomb collisions and adiabatic decompression as the remnant expands. While they are relativistic, adiabatic cooling leads to energy loss on the dynamical timescale of the remnant, $\tau_{\rm ad} \sim R_s/v_s$, where R_s and v_s are the radius and expansion speed of the (assumed spherical) remnant. Once the positrons become non-relativistic, their Coulomb cooling time is short, $\tau_{\rm coul} \sim 3 \times 10^4 (v_+/c) n_0^{-1}$ yr, where v_+ is the positron velocity. Using the analytic expressions for the cooling rates in Furlanetto & Loeb (2002) supplemented by expansion cooling, we have confirmed that the cooling timescales for $\gamma_+ \lesssim 100$ are much shorter than the duration of the Sedov phase. We therefore simply assume that all positrons begin in thermal equilibrium with the shocked ambient gas.

Once the remnant isotropizes, it follows the Sedov (1959) solution until radiative cooling becomes important. Although the remnant is initially asymmetric because of the jet geometry, Ayal & Piran (2001) have shown numerically that even before isotropization, the total volume of the remnant scales with time similarly to a Sedov self-similar blast wave. For this reason, and because $t_{\rm iso}$ is much smaller than the duration of the adiabatic phase, we treat the remnant boundary as a Sedov blast wave throughout both of these phases. Then $R_s = 0.314 (E_{51}/n_0)^{1/5} t_{\rm yr}^{2/5}$ pc, where $t_{\rm yr}$ is the remnant age in years. The adiabatic index of the ambient medium is taken to be $\Gamma = 5/3$.

To calculate $N_+(t)$, we assume that that the positrons are perfectly mixed throughout the interior of the remnant, so that the e^+ density $n_+(r) \propto n_e(r)$, where n_e is the free electron density. We expect such mixing to occur on a timescale $\sim t_{\rm iso}$ or faster because of instabilities on the interface between the SN ejecta and the ambient medium (Chevalier, Blondin, & Emmering(1992); Jun, Jones, & Norman 1996). The annihilation rate is then

$$\dot{N}_+ = -\int_0^{R_s} n_e(r)\, n_+(r) \alpha[T(r)] 4\pi r^2\, dr \qquad (1)$$

where the radial distributions of n_e and T are given by Sedov (1959). Here $\alpha = \alpha_{\rm fa} + \alpha_{\rm Ps}$ is the annihilation rate coefficient with contributions from two channels. The first component, $\alpha_{\rm fa}$, involves direct annihilation with free electrons. In the non-relativistic regime ($T \lesssim 10^8$ K), we use the rate coefficient given by Gould (1989) which includes corrections due to Coulomb focusing. Above this temperature we use the fitting formula given by Svensson (1982). The second coefficient $\alpha_{\rm Ps}$ describes radiative recombination to positronium (Ps) and is given by Gould (1989). Although the corresponding expression is strictly valid only in the non-relativistic regime, Ps formation is sub-dominant for $T_{\rm ann} > 10^6$ K and so the errors introduced by applying it to high temperatures are negligible. The Ps lifetime is $\tau_{\rm Ps} < 1.33 \times 10^{-7}$ sec (depending on the energy level to which recombination occurs), and so we assume that positrons annihilate immediately after forming Ps.

Once the shocked gas cools radiatively to $T \lesssim 10^4$ K, a dense shell begins to form at the shock front. We use the cooling function of Cioffi, McKee, & Bertschinger (1988), for which the nominal shell formation time is $t_{\rm sf} = 3.61 \times 10^4 E_{51}^{3/14} n_0^{-4/7}$ yr. The shell formation process is not fully understood, but two-dimensional simulations have shown it to be both unstable and violent (Blondin et al. 1998). These simulations also find that the dense shell does not fully form until $\sim 1.5 t_{\rm sf}$. We therefore show results up to this time with the caveat that once cooling becomes important at $t_{\rm sf}$ they may no longer be accurate. After shell formation we expect the positrons to annihilate rapidly. Not only does the density of the shell increase dramatically, but also charge exchange with HI comes to dominate as the temperature falls below $\sim 10^5$ K (Bussard, Ramaty, & Drachman 1979; see §4). Thus, we do not expect the annihilation signal to persist after the Sedov phase ends.

Even before shell formation, the loss of energy to cooling radiation decelerates the remnant. We use the analytic approximation of Cioffi et al. (1988) to describe the blast wave size and velocity in this phase (for $t > t_{\rm sf}/e$, where e is Euler's constant). As there is no analytic understanding of the interior structure of the remnant at this stage, we continue to use profiles from the Sedov (1959) solution, normalized to the total size and velocity of Cioffi et al. (1988). Our results are only weakly dependent on the details of these solutions.

3. RESULTS

Figure 3 shows the expected flux of annihilation photons, F_γ, as a function of time for blast waves traveling through media with densities $n_0 = 10^3, 10^2, 10^1, 1$, and 0.1 cm^{-3} (from top to bottom). For each density we carry

the integration through $1.5t_{\rm sf}$. The solid lines show the photon flux from direct annihilation while the dashed lines show that from Ps formation. We scale our results to d_{10}, the remnant distance in units of 10 kpc. The photon production rate is nearly proportional to the ambient density because at a fixed temperature $\tau_{\rm ann} \propto n_e^{-1}$. We find that the average temperature of annihilating positrons is $T_{\rm ann} \approx 1.25T_s$, where T_s is the postshock temperature. The annihilation weighted density is $n_{\rm ann} \approx 2.7n_0$. Both of these formulae are valid to within $\sim 5\%$ for all times and densities. Thus our model finds that most of the annihilations occur in a shell near the shock front. Throughout most of the remnant lifetime, 5×10^5 K $\lesssim T_{\rm ann} \lesssim 10^7$ K. Thus, direct e^+e^- annihilation dominates, with Ps formation becoming important only at late times when the shock velocity has fallen substantially. Note that F_γ is approximately proportional to E_{51}, but the explosion energy also affects $t_{\rm sf}$.

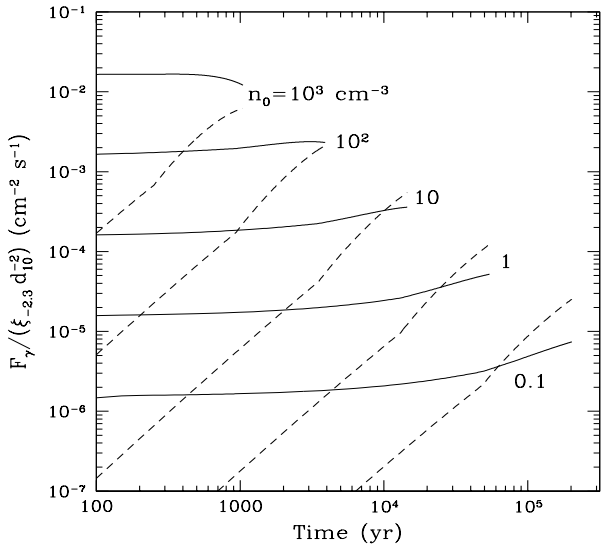

FIG. 1.— Flux of annihilation photons as a function of time for remnants embedded in a medium of density $n_0 = 10^3, 10^2, 10, 1$, and 0.1 cm^{-3}, from top to bottom. Solid curves show the photon flux from free annihilation, while dashed curves show the flux from Ps decay. All results are scaled to a remnant distance $d_{10} = (d/10$ kpc) and assume $E_{51} = 1$.

We next calculate the emission spectrum of the remnant. The spectrum produced by direct annihilation when $k_B T_e \ll m_e c^2$ is given by Svensson, Larsson, & Poutanen (1996). We ignore Coulomb corrections to the annihilation rate, which is a good assumption for the temperatures of interest here (Gould 1989). The decay of Ps is more complicated. One-quarter of the recombinations produce para-Ps, which annihilates into two photons with the spectral distribution given by Gould (1989). Three-quarters of the recombinations produce ortho-Ps, which must decay into three photons in order to conserve angular momentum. The spectrum in this case is a continuum, with a form in the Ps rest frame given by Ore & Powell (1949). We include the broadening due to the thermal motions of the plasma particles by transforming to the observer frame (Bussard et al. 1979) and using the relativistic Maxwell-Boltzmann velocity distribution.[1] In calculating the spectra, we assume for simplicity that all annihilations take place at a single temperature $T_{\rm ann}$. We also neglect the broadening introduced by the expansion speed of the remnant, because the ratio between the thermal e^+ speed and the shock speed is $v_{\rm th}/v_s \sim (m_p/2m_e)^{1/2} \gg 1$, where m_e and m_p are the electron and proton masses.

Snapshots of the annihilation spectrum at $t/t_{\rm sf} = 0.3, 0.6, 0.9, 1.2$, and 1.5 are shown in Figure 3, for media with $n_0 = 1$ cm^{-3} (top panel) and $n_0 = 10^3$ cm^{-3} (bottom panel). As shown in Figure 3, the number of free annihilations per second varies relatively slowly with remnant age, increasing primarily because of the decreasing $T_{\rm ann}$. The line also narrows with time: the full width at half maximum is $\sim 30(T_{\rm ann}/10^7\ {\rm K})^{1/2}$ keV. The line is narrower for lower density media at constant $t/t_{\rm sf}$ because v_s and hence $T_{\rm ann}$ are smaller.

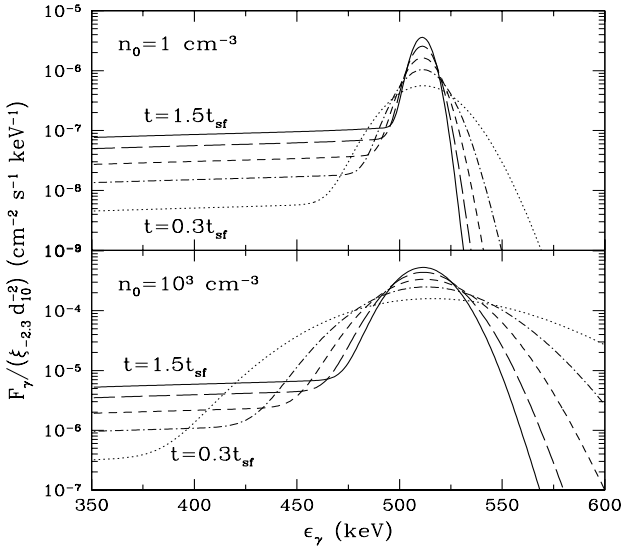

FIG. 2.— Spectral fluxes as a function of photon energy at various times. Results are shown for $n_0 = 1$ cm^{-3} (*top panel*) and $n_0 = 10^3$ cm^{-3} (*bottom panel*) at times $t/t_{\rm sf} = 0.3$ (*dotted curves*), 0.6 (*dot-dashed curves*), 0.9 (*short-dashed curves*), 1.2 (*long-dashed curves*), and 1.5 (*solid curves*). All results are scaled to a remnant distance $d_{10} = (d/10$ kpc) and assume $E_{51} = 1$. The asymmetric line broadening is a property of the annihilation spectrum given by Svensson et al. (1996).

4. DISCUSSION

The BATSE data set implies a GRB rate per comoving volume of $\dot{n}_{\rm iso} \sim 0.5$ Gpc^{-3} yr^{-1}, assuming isotropic emission (Schmidt 2001). The actual event rate is estimated to be larger by an average beaming factor, $\langle f_b^{-1} \rangle \sim 520$ (Frail et al. 2001). Most models associate GRBs with compact stellar remnants; under the assumption that the GRB event rate is proportional to the star formation rate we can convert the above rate density to an event rate per unit mass of star formation (e.g., Porciani & Madau 2001). The expected period between GRB events in the Milky Way is then $\tau_{\rm MW} \sim 3 \times 10^4$ yr $(\dot{n}_{\rm iso}/0.5)^{-1}(\langle f_b^{-1} \rangle/520)^{-1}(R_0/0.007)R_{\rm MW}^{-1}$, where R_0 and $R_{\rm MW}$ are the present day average star formation rates in the universe and in the Milky Way in units of M$_\odot$ Mpc^{-3} yr^{-1} and M$_\odot$ yr^{-1}, respectively, and $\dot{n}_{\rm iso}$ has units of Gpc^{-3} yr^{-1}.

[1]Note, however, that our expression for $\alpha_{\rm Ps}$ does not include relativistic corrections, so our continuum level may be an overestimate at very early times when $T_{\rm ann} \gg 10^8$ K.

Together with Figure 3, this suggests that the positron annihilation line should be detectable from at least one Galactic GRB remnant at any time provided that the circumburst medium has $n_0 \lesssim 1$ cm^{-3}. This conclusion relies on three fortunate coincidences. First and most importantly, the shell formation time satisfies coincidentally $t_{\rm sf} \sim \tau_{\rm MW}$ for $n_0 = 1$ cm^{-3}. Although some fraction of GRBs may occur in dense molecular clouds, recent modeling of jetted afterglows indicates that the ambient density is in the range $n_0 \sim 10^{-3}$–$10^{1.5}$ cm^{-3} (Berger et al. 2000, 2001; Harrison et al. 2001; Panaitescu & Kumar 2001a). Second, in contrast to e^+ created by SNe, GRB positrons annihilate on a timescale $\tau_{\rm ann} \gtrsim t_{\rm sf}$. Third, $T_{\rm ann} \gtrsim 5 \times 10^5$ K, so that a clear line from the direct annihilation channel is visible throughout the source lifetime.

Two backgrounds could contaminate the annihilation line signal. First, relativistic protons accelerated by the collisionless shock can create positrons through the decay of π^+ produced in collisons with thermal protons. Assuming that a fraction ξ_p of the GRB energy is invested in the acceleration of protons (Blandford & Eichler 1987) and using the approximate interaction cross-sections of Mannheim & Schlickeiser (1994), we find that the number of positrons produced before shell formation is $N_{+,\pi} \sim 10^{48} E_{51}^{17/14} n_0^{3/7} (\xi_p/0.1)$ (see Furlanetto & Loeb 2002). Unless $\xi_{-2.3} \lesssim 10^{-6}$, the positron population from this process is negligible compared to that produced in the GRB. A second background is due to inverse-Compton (IC) emission by the electrons accelerated at the shock. The recent detection of TeV γ-ray emission from SN remnants (Tanimori et al. 1998; Muraishi et al. 2000) coupled with the well-observed high-energy synchrotron emission from the same remnants (Koyama et al. 1995, 1997) provides strong evidence for the existence of this population of electrons and calibrates the IC signal. If we extrapolate the observed TeV γ-ray flux to the energy of the annihilation line using the spectral index of the radio synchrotron emission (which should also be the index of the IC spectrum; Reynolds 2001), we find a flux $F_{\gamma,\,\rm IC} \lesssim 10^{-12} d_{10}^{-2} (\epsilon_\gamma/511\ {\rm keV})^{-1.5}$ cm^{-2} s^{-1} keV^{-1}. Thus, the IC background should be negligible compared to the annihilation signal.

The prospects for detection of young GRB remnants in the Milky Way galaxy are good, provided that GRB sources are not confined to dense molecular clouds. As shown in Figure 3, a GRB remnant produces a characteristic annihilation line photon flux of $F_\gamma \sim 3 \times 10^{-5} \xi_{-2.3} n_0/d_{10}^2$ cm^{-2} s^{-1}. The INTEGRAL satellite,[2] expected to be launched in October 2002, will have spectral capabilities in the energy range of interest. For a 10^6 sec observation, its SPI and IBIS instruments have 3σ line sensitivities of $\sim 5 \times 10^{-6}$ cm^{-2} s^{-1} and $\sim 2 \times 10^{-5}$ cm^{-2} s^{-1}, respectively. EXIST,[3] a proposed all-sky hard X-ray survey mission, has an expected 5σ line sensitivity of $\sim 5 \times 10^{-6}$ cm^{-2} s^{-1} in the relevant energy range (assuming an integration time of 10^7 sec, the mean exposure time planned for any point on the sky). These instruments will also have the spectral resolution to identify the line. The IBIS instrument on INTEGRAL and the EXIST survey, with angular resolutions of $12'$ and $5'$ respectively, will also be able to map nearby GRB remnants, for which the angular size at $t_{\rm sf}$ is $\sim 14 E_{51}^{2/7} n_0^{-3/7} d_{10}^{-1}$ arcmin.

If GRBs occur primarily in dense environments, $t_{\rm sf}$ decreases and the probability for observing a remnant declines. Figure 3 shows that the average flux in the annihilation line from a nearby extragalactic source ($d \gtrsim 1$ Mpc) during the Sedov phase will likely remain below the sensitivity limits of the above instruments. However, once shell formation begins, the positrons will annihilate through charge exchange with recombining hydrogen on a timescale $\tau_{\rm cx} \sim 10/(f_{\rm HI} n_{\rm sh})$ yr, where $f_{\rm HI}$ is the neutral fraction (Bussard et al. 1979). If the shell is supported primarily by magnetic and cosmic ray pressure, Cox et al. (1999) find that the shell density at $t_{\rm sf}$ is $n_{\rm sh} \sim 100 B_0^{-1} n_0^{23/14} E_{51}^{1/14}$ cm^{-3}, where B_0 is the transverse component of the ambient magnetic field in units of μG. The maximal annihilation flux is then $F_{\gamma,\rm sh} \sim 3 \times 10^{-3} f_{\rm HI} \xi_{-2.3} E_{51}^{15/14} n_0^{23/14} B_0^{-1} d_{\rm Mpc}^{-2}$ cm^{-2} s^{-1}, where $d_{\rm Mpc}$ is the distance to the GRB in Mpc. Because the charge exchange process produces Ps, 75% of the annihilation energy is released in the continuum, but this suggests that the remnants will brighten significantly during the brief phase of shell formation and may be visible out to the Virgo cluster distance, $d \sim 20$ Mpc. Given the number of galaxies in Virgo, we would therefore expect to find at least one Virgo remnant in this stage provided that $f_{\rm HI} n_{\rm sh} \lesssim 1$ cm^{-3}. The details of the luminosity and spectrum will depend critically on modeling the process of shell formation and cooling. Such modeling stretches the limits of current simulations (e.g., Blondin et al. 1998; Cox et al. 1999) but may become feasible in the future.

We thank J. Raymond for helpful discussions. This work was supported in part by NASA grants NAG 5-7039, 5-7768, and NSF grants AST-9900877, AST-0071019 for AL. SRF acknowledges the support of an NSF graduate fellowship.

[2]See http://astro.estec.esa.nl/SA-general/Projects/Integral/integral.html

[3]See http://exist.gsfc.nasa.gov

REFERENCES

Ayal, S. & Piran, T. 2001, ApJ, 555, 23
Berger, E. et al. 2000, ApJ, 545, 56
Berger, E. et al. 2001, ApJ, 556, 556
Blandford, R. D. & Eichler, D. 1987, Phys. Rep., 154, 1
Blondin, J. M., Wright, E. B., Borkowski, K. J., & Reynolds, S. P. 1998, ApJ, 500, 342
Bloom, J. S. et al. 1999, Nature, 401, 453
Bussard, R. W., Ramaty, R., & Drachman, R. J. 1979, ApJ, 228, 928
Cavallo, G. & Rees, M. J. 1978, MNRAS, 183, 359
Chevalier, R. A., Blondin, J. M., & Emmering, R. T. 1992, ApJ, 392, 118
Cioffi, D. F., McKee, C. F., & Bertschinger, E. 1988, ApJ, 334, 252
Cox, D. P. et al. 1999, ApJ, 524, 179
Dermer, C. D. & Böttcher, M. 2000, ApJ, 534, L155
Djorgovski, S. G., et al. 2001, preprint (astro-ph/0107535)
Frail, D. A. et al. 2001, ApJ, 562, L55
Freedman, D. L. & Waxman, E. 2001, ApJ, 547, 922
Furlanetto, S. R. & Loeb, A. 2002, ApJ, in press (astro-ph/0201313)
Gieseler, U. D. J., Jones, T. W., & Kang, H. 2000, A&A, 364, 911
Gould, R. J. 1989, ApJ, 344, 232
Harrison, F. A. et al. 2001, ApJ, 559, 123
Jun, B., Jones, T. W., & Norman, M. L. 1996, ApJ, 468, L59
Koyama, K. et al. 1995, Nature, 378, 255
Koyama, K. et al. 1997, PASJ, 49, L7

Kulkarni, S. R., et al. 2000, Proc. SPIE, 4005, 9
Loeb, A. & Perna, R. 1998, ApJ, 503, L35
Mannheim, K. & Schlickeiser, R. 1994, A&A, 286, 983
Mészáros, P., Ramirez-Ruiz, E., & Rees, M. J. 2001, ApJ, 554, 660
Milne, P. A., The, L.-S., & Leising, M. D. 1999, ApJS, 124, 503
Muraishi, H. et al. 2000, A&A, 354, L57
Ore, A. & Powell, J. L. 1949, Phys Rev, 75, 1696
Paczynski, B. 2001, Acta Astronomica, 51, 1
Panaitescu, A. & Kumar, P. 2001a, ApJ, 554, 667
————-. 2001b, ApJ, 560, L49
Perna, R., Raymond, J., & Loeb, A. 2000, ApJ, 533, 658
Piran, T. 2000, Phys. Rep., 333, 529
Piran, T. & Ayal, S. 2002, in Disks of Galaxies: Kinematics, Dynamics and Interactions, eds. Athanassoula, E. & Bosma, A., to appear in ASP Conf. Series (astro-ph/0203003)
Piran, T., Kumar, P., Panaitescu, A., & Piro, L. 2001, ApJ, 560, L167
Porciani, C. & Madau, P. 2001, ApJ, 548, 522
Reichart, D. E. 2001, ApJ, 554, 643
Reynolds, S. P. 2001, Space Science Reviews, 99, 177
Rhoads, J. E. 1997, ApJ, 487, L1
Schmidt, M. 2001, ApJ, 552, 36
Sedov, L. I. 1959, Similarity and Dimensional Methods in Mechanics (New York: Academic Press)
Shemi, A. & Piran, T. 1990, ApJ, 365, L55
Suntzeff, N. B. & Bouchet, P. 1990, AJ, 99, 650
Svensson, R., Larsson, S., & Poutanen, J. 1996, A&AS, 120, C587
Svensson, R. 1982, ApJ, 258, 32
Tanimori, T. et al. 1998, ApJ, 497, L25
Thompson, C. & Madau, P. 2000, ApJ, 538, 105
Truelove, J. K. & McKee, C. F. 1999, ApJS, 120, 299
van Paradijs, J., Kouveliotou, C., & Wijers, R. A. M. J. 2000, ARA&A, 38, 379
Woods, E., & Loeb, A. 1999, astro-ph/9907110